International Journal of New Horizons in Physics

http://dx.doi.org/10.18576/ijnhp/030103

Effect of Energetic Argon Ion Irradiation on Microstructure Parameters, Thickness and Refractive Index of ZnSe Films

E. R. Shaaban[1,*], *F. Diab*[2] *and Gamal El-Kashef*[2].

[1]Physics Department, Faculty of Science, Al-Azhar University, P.O. 71452, Assiut - Egypt.
[2]Plasma and Nuclear Fusion Department, Nuclear Research Center, Atomic Energy Authority, Egypt.

Received: 21 Nov. 2015, Revised: 22 Dec. 2015, Accepted: 24 Dec. 2015.
Published online: 1 Jan. 2016.

Abstract: The effect of distance of energetic argon ion irradiation is studied on ZnSe stoichiometric film having compressive lattice strain and improve the refractive index. An increase in grain size and decrease in lattice strain was observed with decreasing irradiation distance (or increasing ion energy). The decrease in distance of energetic argon ion irradiation can effectively improve the transmittance. Both of film thickness and refractive index were calculated in terms of Swanepoel's method with high precision. The film thickness and refractive index of ZnSe thin films decrease with increasing the energetic argon ion irradiation i.e. decrease the distance between the anode and the sample.

Keywords: ZnSe; thin film; XRD; irradiation distance; Plasma focusing.

1 Introduction

Zinc selenide (ZnSe) is an attractive of II-VI Semiconductor compounds because of their specific optoelectronic device applications [1]. ZnSe thin films is very important for fabricating and developing the need of the integrated circuit industry [2]. The requirement for development of the smallest devices with higher speed especially in new generation of integrated circuits requires advanced materials and new processing techniques suitable for future giga scale integration (GSI) technology [3, 4]. So, recent studies have revived interest in ZnSe films [5-10].. These reports show the variation of optical properties of ZnSe film as a function of film parameters like its thickness, deposition rate, substrate temperature, effect of heat-treatment etc. The optical properties were shown to have a strong correlation with the microstructure parameters [5]. The mentioned devices related to ZnSe can be fabricated in terms of thin-film technology these method include, thermal evaporation under vacuum, pulsed-laser deposition, molecular beam epitaxy, electrodeposition, and spray pyrolysis [11-14]. Moreover, the studying of the structural and optical properties of ZnSe thin film gives valuable information about the ZnSe properties. A lot of publications have been determined both refractive index and thickness of thin films in terms of double beam spectrophotometer and optical spectroscopic ellipsometry (OSE). In view of the potential applications in surface science [15] and integrated electronics[16], studies on ion beam effects and plasma processing have gained significance in recent years. Desired and controlled modifications of physical and surface properties have been reported on ion irradiation [17]. Material modification such as structure parameter optical properties, etc, can be achieved by bombarding material with radiation or highly kinetic ions (plasma). This manuscript details the modification crystallize size, lattice strain, film thickness and refractive index by plasma irradiation with highly energetic argon ions.

2 Experimental

High purity ZnSe powder (99.999 %) from Aldrich Company was used for preparation of ZnSe thin films with thickness about 925 nm onto ultrasonically cleaned glass substrate kept at constant temperature (373 K) using a thermal evaporation unit (Denton Vacuum DV 502 A) under vacuum of 10^{-6} Pa. In order to obtain the optimal conditions for a homogeneous thin film, a mechanical rotation of the substrate holder (≈30 rpm) during deposition was used. Both the film thickness and the deposition rate were controlled using a quartz crystal monitor DTM 100. The deposition rate was kept at 2 nm/s during the preparation of thin films. The experimental setup of the present plasma focusing device is shown in Fig. 1. The system is energized by a capacitor bank consists of four capacitor which are connected in parallel and has a total capacitance of 30.84 μf and charged up to 8 KV giving a peak discharge current up to 150 kA. To initiate the discharge through the electrodes a high voltage trigger was located near the spark gap which is a vital element since it is responsible to start the breakdown just before the shots.

*Corresponding author e-mail: esam_ramadan2008@yahoo.com

The cleaning process of the spark gap is carried out before and after 5 shots. The discharge chamber is made of stainless steel and has a length of 40 cm and diameter of 38 cm.

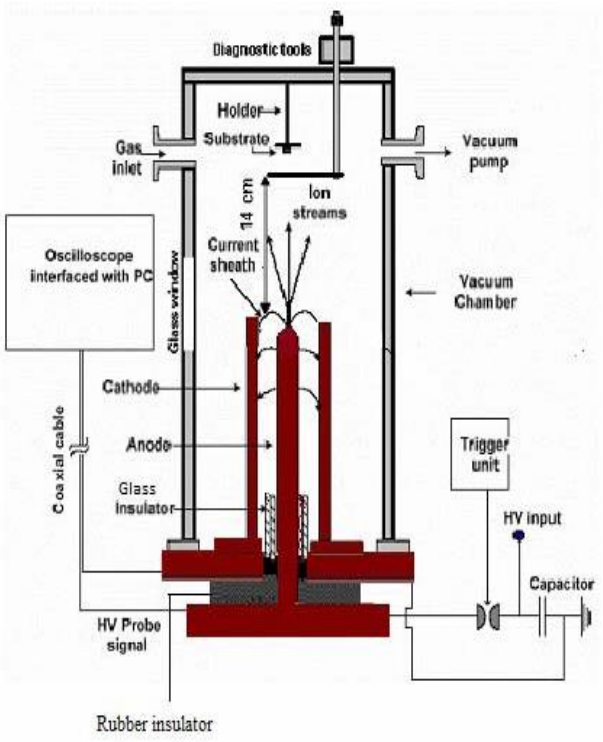

Fig. 1: Schematic of experimental setup for PF device.

Moreover, the electrodes of the plasma focus device in this experiment are a solid cylindrical tube to a void the excessive hard x-ray emission from the anode surface due to electron bombardment. The plasma focus is operated with argon as the working gas. The device was evacuated to lower than 10^{-2} Pa before puffing Argon gas by rotary van pump) and filled with the required gas (argon) to a particular pressure (0.2–2 Pa) before operation. This level of vacuum proved to be sufficient for operating with good focus in argon gas. A shutter was placed between the aperture and the film sample to avoid exposing the sample to weak ion beams produced while optimizing the PF device for strong focusing. The shutter was removed after optimum focus was achieved, thereby exposing the sample to energetic ions in the next PF pulse. By varying the distance (extended from 16 to 7 cm) of the film from the anode, the average kinetic energy of argon ions impinging the film can be varied. The structure of ZnSe powder and both as grown film and plasma irradiated film were examined by X-ray diffraction (XRD) (Philips X-ray diffractometry (1710)) with Ni-filtered CuK_α radiation with (λ = 0.15418 nm). Both the morphology the elemental composition of the as grown and plasma irradiated film were analyzed by using energy dispersive X-ray spectrometer unit (EDXS) interfaced with a scanning electron microscope, SEM (JOEL XL) operating an accelerating voltage of 30 kV. The relative error of determining the indicated elements does not exceed 2 %. The measurements of the transmittance, *T* were carried out in terms of a double-beam spectrophotometer (Jasco V670) at normal incidence of light in a wavelength (λ) range between 400 and 2500 nm. The measured transmittance spectrum were carried out without a glass substrate in the reference beam in order to calculate the refractive index and the film thickness of ZnSe thin films according to Swanepoel's method.

3 Results and Discussion

3.1 The crystallographic structure of ZnSe thin films

Fig. 1 displays XRD diffractogram of ZnSe powder according to JCPDS Data file no.: 05-0566, it can be indexed to ZnSe cubic phase with polycrystalline in nature. The X-ray diffraction of as grown and plasma irradiated of ZnSe films are shown in Fig. 2. Our X-ray diffraction data agrees quite well with the powder diffraction data JCPDS card 05-0566.

The observed peaks of as grown and plasma irradiated of ZnSe films are polycrystalline with peaks detected at 2θ = 28.56º, 47.52º and 56.29º corresponding to C(1 1 1), C(2 2 0) and C(3 1 1) orientations, respectively.

Fig. 2 shows that the intensities of the peaks decrease with increasing the energetic argon ion irradiation (i.e. reduction of distance) but the full width at half maximum (FWHM) increases with increasing energetic argon ion irradiation of ZnSe films. The lattice strain (ε) parameter is calculated using the following relation [18, 19]

$$\varepsilon = \frac{\beta}{4\tan(\theta)} \quad (1)$$

Where θ is the Bragg's diffraction angle of the peak and β is the breadth of the peak. β describes the structural broadening, which is the difference in integral X-ray peak profile width between the sample, β_{obs} and a standard (silicon), which is given by

$$\beta = \sqrt{\beta_{obs}^2 - \beta_{std}^2}\ . \quad (2)$$

Also, from XRD patterns, the crystallite size of films was calculated by using

the well-known Debye –Scherrer's formula [18-20]

$$D_v = \frac{k\lambda}{\beta\cos(\theta)} \quad (3)$$

Where λ is the wavelength (1.54 Å). Fig. 3 shows a

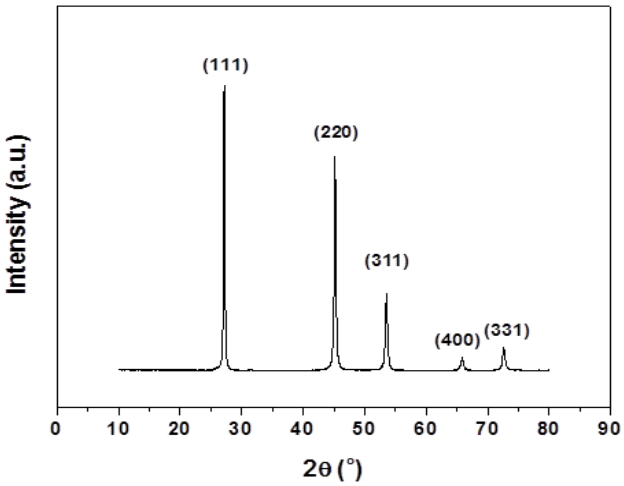

Fig. 2: X-ray diffraction spectra of ZnSe powder

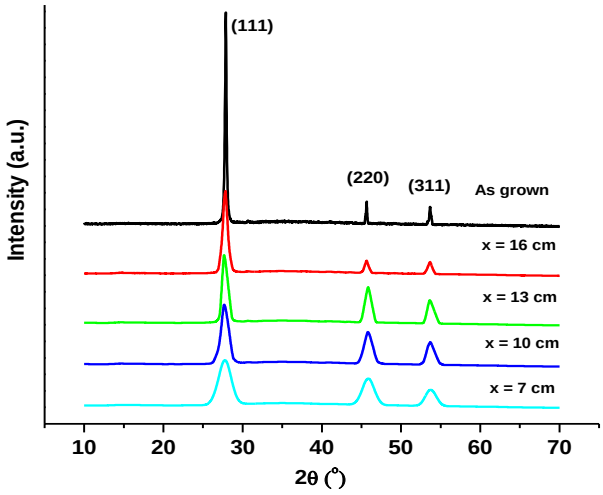

Fig. 3:X-ray diffraction of as-grown of ZnSe film, and films irradiated at x = 16, 13, 10, 7 cm from the anode.

comparative look of microstructure parameters (D_v and ε) as a function of argon plasma ion irradiation distance (7, 9, 11, 13 and 15 cm). An increasing in crystallite size and a decrease in lattice strain were observed with increasing irradiation distance extend from 7 to 16 cm (or decreasing ion energy). This shows that plasma ions break the grains into smaller sizes depending on their energy or distance. But the increasing in the lattice strain reflects the increasing in the concentration of lattice imperfections due to increasing irradiation distance (decreasing ion energy) which causes the increase of FWHM thus increase in crystallize size [21-25].

3.2 Spectrophotometric analysis

Fig. 4 displays the variation of absolute value of transmittance, T against λ of different distance of argon plasma ion irradiation of ZnSe thin films. In a wide spectral range extended from λ = 400 nm to λ = 2500 nm, the transmission spectrum showed an interference fringes in both transparent region and medium absorption region. As we approach to the lower wavelengths where the absorption starts to occur and the intensity of the interference fringes starts to shrink gradually until it reach to the strong absorption region. Fig. 4 also shows an important feature of increasing (improving) the transmittance spectra with increasing the energetic irradiation of argon plasma ion (i.e decreasing the distance between anode and the sample).

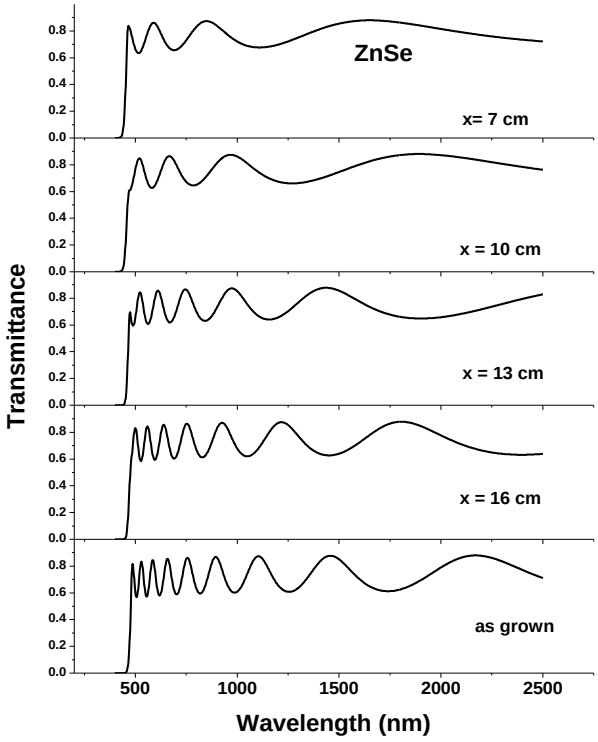

Fig. 4: Typical transmission spectrum for as grown and films irradiated at x = 16, 13, 10, 7 cm from the anode.

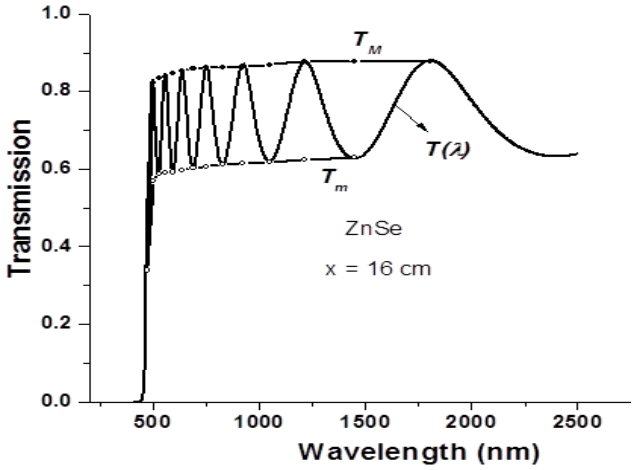

Fig. 5: The typical transmission spectra for an irradiated of ZnSe film at x =16 cm. Curves T_M, T_m, according to the text.

The refractive index was determined in terms of envelope method, which suggested by Swanepoel. This method based on the recording envelopes around the interference maxima

Table 1. Values of λ, T_M and T_m for as-grown of ZnSe film, and films irradiated at x = 16, 13, 10 and 7 cm from the anode. The calculated values of refractive index and film thickness are based on the Swanepoel's method.

Sample	λ	T_M	T_m	s	n_1	d_1 (nm)	m_0	m	d_2 (nm)	n_2
As grown										
	530	0.8583	0.5722	1.559	2.588	0	9.08	9	922	2.628
	556	0.8594	0.5749	1.555	2.576	975	8.61	8.5	917	2.603
	586	0.8607	0.5783	1.551	2.561	978	8.12	8	915	2.582
	618	0.862	0.5815	1.547	2.547	957	7.66	7.5	910	2.553
	658	0.8635	0.585	1.543	2.532	933	7.15	7	910	2.537
	702	0.865	0.5884	1.538	2.517	926	6.66	6.5	906	2.514
	756	0.8667	0.5922	1.533	2.501	912	6.15	6	907	2.499
	818	0.8684	0.5959	1.528	2.485	920	5.65	5.5	905	2.478
	894	0.8702	0.599	1.522	2.471	918	5.14	5	905	2.462
	986	0.872	0.6019	1.517	2.458	900	4.63	4.5	903	2.444
	1106	0.8739	0.6056	1.511	2.442	901	4.1	4	906	2.437
	1254	0.8756	0.6083	1.506	2.43	916	3.6	3.5	903	2.418
	1460	0.8773	0.6087	1.501	2.427	918	3.09	3	903	2.413
	1740	0.8787	0.6089	1.496	2.424	0	2.59	2.5	897	2.396
		$\bar{d}_1 = 929$ nm		$\sigma_1 = 26.6$ nm (2.9 %)		$\bar{d}_2 = 908$ nm			$\sigma_2 = 6.5$ nm (0.7 %)	
x = 16 cm										
	558	0.8595	0.5902	1.555	2.517	0	7	7	776	2.538
	596	0.8611	0.5923	1.55	2.507	821	6.53	6.5	773	2.518
	638	0.8628	0.5965	1.545	2.49	792	6.06	6	769	2.488
	690	0.8646	0.6019	1.539	2.467	774	5.55	5.5	769	2.466
	752	0.8666	0.6064	1.533	2.449	771	5.06	5	768	2.443
	830	0.8687	0.6109	1.527	2.43	777	4.54	4.5	769	2.427
	924	0.8708	0.6146	1.52	2.414	781	4.06	4	766	2.402
	1048	0.873	0.6185	1.514	2.397	758	3.55	3.5	765	2.384
	1216	0.8752	0.6242	1.507	2.374	749	3.03	3	768	2.371
	1452	0.8773	0.6299	1.501	2.352	764	2.51	2.5	772	2.359
	1804	0.8789	0.6323	1.496	2.342	0	2.02	2	770	2.345
		$\bar{d}_1 = 776$ nm		$\sigma_1 = 21$ nm (2.7 %)		$\bar{d}_2 = 769$ nm			$\sigma_2 = 3.1$ nm (0.4%)	
x = 13 cm										
	520	0.8578	0.6036	1.56	2.469	0	6.02	6	632	2.491
	562	0.8597	0.6068	1.554	2.455	657	5.54	5.5	629	2.468
	610	0.8617	0.6124	1.548	2.433	643	5.06	5	627	2.436
	670	0.8639	0.619	1.541	2.406	636	4.56	4.5	627	2.408
	744	0.8663	0.6251	1.534	2.382	631	4.06	4	625	2.376
	842	0.869	0.6312	1.526	2.357	622	3.55	3.5	625	2.353
	974	0.8718	0.6367	1.517	2.335	625	3.04	3	626	2.333
	1158	0.8745	0.6416	1.509	2.315	632	2.54	2.5	625	2.312
	1432	0.8771	0.6454	1.501	2.299	629	2.04	2	623	2.287
	1898	0.8792	0.6485	1.495	2.286	0	1.53	1.5	623	2.273
		$\bar{d}_1 = 634$ nm		$\sigma_1 = 11$ nm (1.7 %)		$\bar{d}_2 = 626$ nm			$\sigma_2 = 2.8$ nm (0.5 %)	
x = 10 cm										
	518	0.8577	0.6245	1.56	2.393	0	4.03	4	433	2.426
	582	0.8606	0.6267	1.552	2.382	454	3.57	3.5	428	2.385
	668	0.8639	0.6348	1.542	2.35	432	3.07	3	426	2.347
	786	0.8675	0.6457	1.53	2.308	430	2.56	2.5	426	2.301
	968	0.8716	0.6531	1.518	2.278	427	2.05	2	425	2.267
	1276	0.8758	0.6591	1.505	2.254	0	1.54	1.5	425	2.241
		$\bar{d}_1 = 436$ nm		$\sigma_1 = 12$ nm (2.8 %)		$\bar{d}_2 = 427$ nm			$\sigma_2 = 3.1$ nm (0.7 %)	
x = 7 cm										
	590	0.8609	0.6498	1.551	2.3	0	2.99	3	385	2.306
	696	0.8648	0.6583	1.539	2.267	393	2.5	2.5	384	2.267
	850	0.8692	0.6671	1.525	2.233	383	2.02	2	381	2.215
	1124	0.8741	0.6776	1.51	2.193	376	1.5	1.5	384	2.196
	1640	0.8783	0.6968	1.497	2.127	0	0.996	1	386	2.136
		$\bar{d}_1 = 384$ nm		$\sigma_1 = 8.8$ nm (2.3 %)		$\bar{d}_2 = 383$ nm			$\sigma_2 = 1.9$ nm (0.5 %)	

and minima of the transmittance spectra [39-41]. Fig. 5 illustrates the measured transmittance spectra of ZnSe thin films at distance x = 13 cm from the anode. As shown in Fig. 5 the number of interference fringes was the highest for as grown ZnSe sample and decrease at distance x = 16 and continuous to decrease gradually with decreasing the distance between the sample and the anode, i.e. the transmittance improve with increasing argon plasma irradiation energy. According envelope method, the value of refractive index can be calculated at a determined wavelength in terms of the relationship

$$n = \left[N_1 + (N_1^2 - s^2)^{\frac{1}{2}} \right]^{\frac{1}{2}} \quad (3)$$

Table 2: Film thickness, broadening, *β, crystallize size, lattice strain and* Cauchy coefficient for as-grown of ZnSe film, and films irradiated at x = 16, 13, 10 and 7 cm from the anode.

Sample *distance*	***Thickness (nm)***	***β(after correction)***			***D_v (nm)***	***ε x10^{-3}***	**Cauchy coefficient**	
		(1 1 1)	**(2 2 0)**	**(3 1 1)**			B	A x10^4
7	383	0.787	0.948	0.977	13.68	2.35	2.133	6.435
10	427	0.547	0.616	0.661	18.82	1.16	2.236	6.001
13	626	0.353	0.421	0.419	28.64	0.74	2.259	6.616
16	769	0.253	0.297	0.300	39.94	0.51	2.326	6.690
as grown	729	0.181	0.217	0.213	55.21	0.35	2.377	6.939

Where

$$N_1 = 2s\frac{T_M - T_m}{T_M T_m} + \frac{s^2+1}{2}$$

where T_M and T_m, are the transmittance maximum and the corresponding minimum at the same wavelength λ. Alternatively, one of these values is an experimental interference extreme and the other one is derived from the corresponding envelope; both envelopes were extracted by using the program Origin version 7 (OriginLab Corp.) see Fig. 5 (a, b). On the other hand, the refractive index of substrate was calculated in terms of the well-known relationship

$$s = \frac{1}{T_s} + \left(\frac{1}{T_s} - 1\right)^{\frac{1}{2}} \quad (4)$$

Where T_s is the transmission of the substrate. Moreover, the film thick was calculated using the following equation

$$d = \frac{\lambda_1 \lambda_2}{2\left(\lambda_1 n_{e2} - \lambda_2 n_{e1}\right)} \quad (5)$$

Where n_{el} and n_{e2} are the refractive indices at two adjacent maxima (or minima) at λ_1 and λ_2. The values of film thickness of as grown of ZnSe film and and films irradiated at x = 16, 13, 10 and 7 cm from the anode are listed in table 2.

It observed that the film thickness decrease with increasing the argon plasma irradiation sample (reduction in distance). For all investigated films the refractive index *n* decreases with increasing the wavelength showing normal dispersion following two-term Cauchy dispersion relationship, $n(\lambda) = A + B/\lambda^2$, which can be used for extrapolation the whole wavelengths [38] as shown in Fig. 7**.** In terms of the least squares fit between *n* versus $1/\lambda^2$, the values of A and B can be extracted and listed in table 1. Fig. 6 showed that the values of refractive index decrease with increasing the argon plasma irradiation (i. e increasing the distance between the anode and the sample) due to improvement in transmittance spectrum.

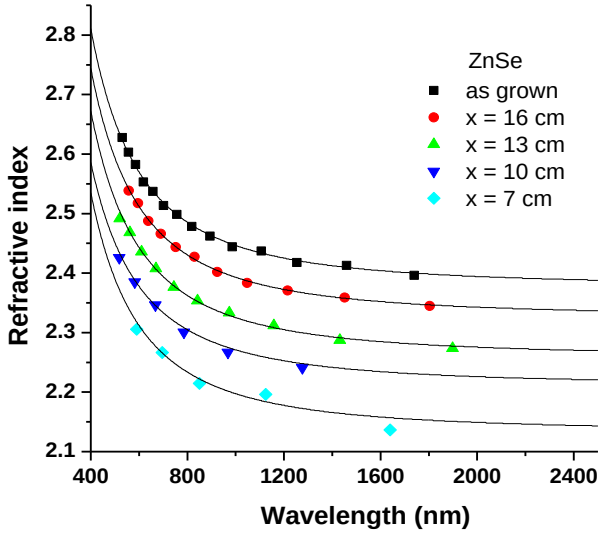

Fig. 6: Refractive index dispersion spectra for ZnSe films for as grown and films irradiated at x = 16, 13, 10, 7 cm from the anode.

4 Conclusions

The microstructure parameters, crystallize size and lattice strain were determined for as-grown of ZnSe film, and films irradiated at x = 16, 13, 10 and 7 cm from the anode. An increasing in crystallite size and a decrease in lattice strain were observed with increasing irradiation distance extend from 7 to 16 cm (or decreasing ion energy). This shows that plasma ions break the grains into smaller sizes depending on their energy or distance. But the increasing in the lattice strain reflects the increasing in the concentration of lattice imperfections due to increasing irradiation distance (decreasing ion energy) which causes the increase of FWHM thus increase in crystallize size. Both film thickness and refractive index were determined for for as-grown of ZnSe film, and films irradiated at x = 16, 13, 10 and 7 cm from the anode. It observed that the film thickness decrease with increasing the argon plasma irradiation sample (reduction in distance). Also the values of refractive index decrease with increasing the argon plasma irradiation (i. e increasing the distance between the anode and the sample) due to improvement in transmittance spectrum.

References

[1] J. J. Zhu, Y. Koltypin and A. Gedanken, *Chem. Mater.* **12 (1)** (2000), p. 73.

[2] L. Eckertová, *Physics of Thin Films, Springer Science & Business Media* (2012).

[3] M. P. Valkonen, S. Lindroos, M. Leskela and *Appl. Surf. Sci.* **134** (1998), p. 283.

[4] I. T. Sinaoui, F. Chaffar Akkar, F. Aousgi and M. Kanzari, *Int. J. Thin Fil. Sci. Tec.* **3, No. 1** (2014), p. 19.

[5] E. R. Shaaban, *J .Alloys Compd. 563 (2013) 274-279.*

[6] S. Zhao, F. Ma and Z. Song, *Optical Materials* **30** (2008), p. 910.

[7] K. Luo, S. Zhou and L. Wu, *Thin solid films* **517** (2009), p. 5974.

[8] P. Eiamchai, P. Chindaudom, A. Pokaipisit and P. Limsuwan, *Current Applied Physics* **9** (2009), p. 707.

[9] J. Park, J. Kook and Y. Kang, *Bull. Korean Chem. Soc* **31** (2010), p. 397.

[10] N. Khemiri, B. Khalfallah, D. Abdelkader and M. Kanzari, *Int. J. Thin Fil. Sci. Tec.* **3, No. 1** (2014), p. 7.

[11] E.R. Shaaban, M. Abdel-Rahman, El Sayed Yousef and M. T. Dessouky, *Thin Solid Films* **515** (2007), p. 3810

[12] Y.P. Venkata Subbaiah, P. Prathap, M. Devika and K. T. R. Reddy, *Physica B:* **365** (2005), p. 240.

[13] S. Lalitha, R. Sathyamoorthy, S. Senthilarasu, A. Subbarayan and K. Natarajan, *Solar Energy Materials & Solar Cells* **82** (2004), p. 187.

[14] Y. Ni, G. Yin, J. Hong and Z. Xu, *Mater. Res. Bull* **39** (2004), p. 1967.

[15] U. Gerlach and O. Meyer, *Surf. Sci. 103, 534 (1981).*

[16] T. A. Skotheim, R. L. Elsenbaumer and J. R. Reyxold, *"Handbook of conducting polymers", (New York; Marcel Dekker)1998, p 589-638.*

[17] M. A. Loudiana, A. Soamid and J. T. Dickinson, *Surf. Sci. 141, 409 (1986).*

[18] B. D. Cullity, *Elements of X-ray diffraction. 2nd ed. London: Addition-Weasley; 1978.*.

[19] J.I. Langford and A. J. C. Wilson, *J. Appl. Cryst. 11 (1978) pp 102-113.*

[20] E. R. Shaaban, M. El-Hagary, M. Emam-Ismail, A. Matar and I. S. Yahia, *Mater. Sci. Eng., B* **178** (2013), p. 183.

[21] G. K. Williamson and H. W. Hall, *Acta Metallurgica* **1** (1953), p. 22.

[22] D.G. Morris, M. A. Morris and M. LeBoeuf, *Materials Science and Engineering A* **156** (1992), p. 11.

[23] G. H. Chen, C. Suryanarayana and F. H. Froes, *Metallurgical and Materials Transactions* **26A** (1995), p. 1379.

[24] E. Szewczak, J. Paszula, A. V. Leonov and H. Matyja, *Materials Science and Engineering A* **A226-228** (1997), p. 115.

[25] E. R. Shaaban, *J. Alloys Compd* **563** (2013), p. 274.

[26] E. R. Shaaban, *Mat. Chem. Phys.* **100** (2006), p. 411.

[27] S. Chaudhuri, S. K.Biswas, A. Choudhury and *J. Mater. Sci.* **23** (1988), p. 4470.

[28] B.A. Mansour, H. Shaban, S. A. Gad, Y. A. EL-Gendy and A. M. Salem, **6** (2010), p. 13.

[29] E. Szewczak, J. Paszula, A. V. Leonov and H. M. , *Materials Science and Engineering B* **A226-228** (1997), p. 115.

[30] M. Kastner, *Physical. Review Letter* **28** (1972), p. 355.

[31] L. L. K. (Ed.), *Polycrystalline and Amorphous Thin Films and Devices, Academic Press, New York* (1980), p. 135.

[32] E. R. Shaaban, M. F. Kaid, E. Moustafa and A. Adel, *J. Physics. D:* **41** (2008), p. 53125301.

[33] E. R. Shaaban, Y. A. M. Ismail and H. S. Hassan, *J. Non-Cryst. Solids* **376** (2013), p. 61.

[34] M. Nowak, *Thin Solid Films* **266** (1995), p. 258.

[35] J. I. Pankove and , *Optical Processes in Semiconductors, Dover, New York, (1971) 44.*

[36] E.A. Davis and N. F. Mott, *Philos. Mag.* **22** (1970), p. 903.

[37] E. R. Shaaban, M. A. Kaid and M. G. S. Ali, *J. Alloys Compd.* **613** (2014), p. 324.

[38] E. Márquez, J. M. González-Leal, A.M. Bernal-Oliva, R. Jiménez-Garay, T. Wagner and 503., *J. Non-Cryst. Solids* **354** (2008), p. 503.

[39] E. R. Shaaban, *Mater. Chem. Phys.* **100** (2006), p. 411.

[40] R. Swanepoel, *J. Physics E* **16** (1983), p. 121.

[41] E. R. Shaaban, *Appl. Phys. A* **115** (2014), p. 919.

[42] N. Revathi, P. Prathap, K.T. Ramakrishna Reddy and *Solid State Science* **11** (2009), p. 1288.

[43] S.H. Wemple and M. DiDomenico, *Phys. Rev. B* **3** (1971), p. 1338.